LIMNOLOGY and OCEANOGRAPHY: METHODS

ASLO

Limnol. Oceanogr.: Methods 19, 2021, 303–316

doi: 10.1002/lom3.10424

A new method to estimate planktonic oxygen metabolism using high-frequency sensor measurements in mesocosm experiments and considering daytime and nighttime respirations

Tanguy Soulié,[1]* **Sébastien Mas**,[2] **David Parin**,[2] **Francesca Vidussi**,[1] **Behzad Mostajir**[1]

[1]MARBEC (MARine Biodiversity, Exploitation and Conservation), Univ Montpellier, CNRS, Ifremer, IRD, Montpellier, France
[2]MEDIMEER (Mediterranean Platform for Marine Ecosystems Experimental Research), OSU OREME, CNRS, Univ Montpellier, IRD, IRSTEA, Sète, France

Abstract

Understanding how aquatic ecosystems respond to perturbations has emerged as a crucial way to predict the future of these ecosystems and to assess their capacity to produce oxygen and store atmospheric carbon. In this context, in situ mesocosm experiments are a useful approach for simulating disturbances and observing changes in planktonic communities over time and under controlled conditions. Within mesocosm experiments, the estimation of fundamental parameters such as gross primary production (GPP), net community production (NCP), and respiration (*R*) allows the evaluation of planktonic metabolic responses to a perturbation. The continuous estimation of these metabolic parameters in real time and at high frequency is made possible by employing noninvasive automated sensors in the water column. However, some uncertainties and methodological questions about the estimation of daytime respiration remain to be addressed for this method, and notably to address the fact that respiration could be significantly higher during the day than during the night. In this study, data from two in situ mesocosm experiments performed in fall and spring in a coastal Mediterranean area were used to develop a new method of estimating daytime respiration, and in turn daily GPP, *R*, and NCP, by considering the maximum instantaneous *R*, and that takes into account the variability of the coupling between day–night and dissolved oxygen cycles. This new method was compared with the Winkler incubation technique and with another existing method. Results showed that using this existing method, daytime *R* was significantly underestimated relative to estimates obtained with the newly proposed method.

Aquatic ecosystems undergo many perturbations at different temporal and spatial scales due to natural and anthropogenic factors. Understanding how these perturbations affect these ecosystems is crucial for predicting their future status. Due to their importance in global biogeochemical cycles and in aquatic ecosystem functioning, assessing the response of planktonic communities to various environmental disturbances is therefore of great importance and interest. To do so, mesocosm experiments are experimental units that can be used to simulate disturbances and observe changes in the studied community over time and under controlled conditions while ensuring the reproducibility of the tested perturbations (Stewart et al. 2013; Dzialowski et al. 2014). They closely simulate the natural environment and therefore constitute a link between laboratory and field observations (Odum 1984; Crossland and Point 1992).

Changes in the metabolic processes associated with planktonic communities indicate the response of these communities to disturbances; therefore, measuring metabolic parameters during mesocosm experiments is essential, and there is a need to obtain reliable estimates of these parameters. Some of these metabolic parameters that are related to oxygen, such as gross primary production (GPP), which is the autotrophic production of oxygen through the conversion of inorganic carbon to organic carbon, and aerobic respiration (R), which is the consumption of oxygen through the oxidation of organic carbon to inorganic carbon by both autotrophic and

*Correspondence: tanguy.soulie@gmail.com

Author Contribution Statement: B.M. and F.V. conceived the study. B.M., F.V., and S.M. designed and managed the mesocosm experiments. D.P. set up the sensor system and retrieved the sensor data. T.S. and S.M. calibrated the sensors. T.S. processed the sensor data, performed all the analyses, and wrote the original draft of the article, with the input of B.M., F.V., and S.M.

Additional Supporting Information may be found in the online version of this article.

heterotrophic organisms, are of great importance in understanding and managing aquatic ecosystems (Hanson et al. 2008). Indeed, the net community production (NCP), which is the difference between GPP and *R*, represents the balance between anabolic and catabolic processes and thus between autotrophy and heterotrophy (Staehr et al. 2012).

Due to their importance in understanding the functioning of aquatic ecosystems, these metabolic parameters have been estimated for more than half a century using various methods. The Winkler incubation method, which is the reference method, consists of light and dark incubations of natural samples in small glass bottles for a certain interval of time. The production of dissolved oxygen (DO) in the light bottles and its consumption in the dark bottles is determined by titration with the Winkler technique (Winkler 1888). Another technique used to estimate metabolic parameters is measuring the diel free-water changes in the DO concentration over a certain period of time (Odum 1956). Oviatt et al. (1986) proposed estimating the net production from dawn to dusk and the respiration from dusk to the following dawn. More recently, Kritzberg et al. (2014) obtained GPP, R, and NCP with four DO measurements over a 24 h period.

Additionally, submersible automated DO sensors, that provide high-frequency DO measurement data allowing for real-time observations at intervals of every minute to every hour, can be used to assess metabolic parameters. These sensors can be deployed for a long period and in remote locations and are traditionally used on buoys and gliders to monitor key environmental parameters, at various time scales and for different aquatic systems. They have enabled a better understanding of the trends in the physical and biological variables in these systems and have even provided new insights into ecosystem functioning (de Eyto et al. 2019; Trombetta et al. 2019). Within the framework of mesocosm experiment, using sensor data to estimate metabolic parameters has several advantages compared to the traditional incubation technique, as the sensors are noninvasive and their use does not introduce bottle or container effects into the measurement, thus avoiding the error propagation associated with incubations (Staehr et al. 2010*a*). Moreover, ecologically important short-timescale temporal changes in the DO can easily be monitored with sensors but are not detected by the Winkler incubation method.

Despite its advantages, only a few studies have used the free-water method of estimating metabolic parameters in mesocosm experiments, and even fewer studies have used high-frequency sensors to assess metabolic parameters in mesocosm experiments (Oviatt et al. 1984, 1986; Brinkman et al. 1995; Leclercq et al. 1999; Whitledge and Rabeni 2000; Mostajir et al. 2013; Reijo et al. 2018; Hensley and Cohen 2020). Because of the substantial technical constraints, estimating oxygen-related metabolic parameters using high-frequency sensors in mesocosm experiments is still not widespread in the scientific community. However, high-frequency sensors have been commonly used to estimate oxygen metabolic parameters in the field, especially in lake studies (Van de Bogert et al. 2007; Hanson et al. 2008; Staehr et al. 2010*b*; Alkire et al. 2012; Wikner et al. 2013; Briggs et al. 2018; Demars et al. 2018).

Due to the limited number of studies that have used high-frequency DO data to estimate metabolic parameters in mesocosm experiments, there are still some methodological questions regarding the use of this technique and the reliability of the metabolic estimates derived from it. The main uncertainty is related to the estimation of respiration occurring during the day (Rdaytime). For simplicity, Rdaytime has been assumed to be equal to the R that occurs at night (Rnight) in most field studies using sensor data to derive planktonic respiration rate (Hanson et al. 2003; Lauster et al. 2006; Staehr et al. 2010*a*), despite increasing evidence that Rdaytime is significantly greater than Rnight, for example, up to 640% higher at the beginning of the night than that at the end of it (Markager et al. 1992; Xue et al. 1996; Pringault et al. 2007; Carvalho and Eyre 2012). Indeed, previous studies have reported that respiration is enhanced by photosynthesis and the resultant photosynthetic products (Markager and Sand-Jensen 1989; Markager et al. 1992; Mantikci et al. 2017), with postillumination rates 50–340% higher than dark respiration levels (Beardall et al. 1994; Hotchkiss and Hall 2014). The calculation of Rdaytime has been proposed to be done just after sunset, when autotrophic respiration still relies on the photosynthetic products accumulated during the daylight period (Mostajir et al. 2013). Nevertheless, the method of Mostajir et al. (2013) does not consider the fact that the DO cycle does not strictly follow the day–night cycle. Indeed, this method assumes that the DO concentration starts to decrease at sunset; however, this decrease can start earlier if respiration is stronger than production even when there is still daylight. This mismatch can be caused by various environmental factors, including the amount of light available for photosynthesis and the water temperature, which affects metabolic processes. Hence, it seems clear that considering a period starting at sunset for the calculation of Rdaytime may yield very different estimates for days when the cycle of oxygen matches the light cycle and days when the cycles do not match. Therefore, there is a need to establish a method that considers this variability in the calculation of Rdaytime.

Accordingly, a new method to estimate Rdaytime using high-frequency DO data from enclosed mesocosm experiments that takes into account the potential variability between DO and day–night cycles is provided in this investigation. In addition, the metabolic estimates obtained with this new method were compared with those obtained with the method of Mostajir et al. (2013) and with the Winkler incubation technique. Moreover, a comparison was performed between two time periods used for the daily integration of daytime and night respiration estimates. Overall, this new method is based on data obtained during two in situ enclosed

mesocosm experiments conducted in a Mediterranean coastal shallow lagoon in fall 2018 and spring 2019.

Materials and procedures

Experimental setup

Mesocosm experiments

Two mesocosm experiments were carried out in Thau Lagoon, which is a productive shallow (4 m mean depth) coastal lagoon located in the western Mediterranean in southern France. The experiments lasted 15 d in October 2018 (Exp. 1) and 17 d in May and June 2019 (Exp. 2). In this article, data from three mesocosms in Exp. 1 (Oct 01, Oct 02, and Oct 03) and three mesocosms in Exp. 2 (Jun 01, Jun 02, and Jun 03) were used. As an example, Oct 01 refers to the data set obtained for one of the three replicates mesocosms of the Exp. 1 which took place in October 2018.

The mesocosms were established at the Mediterranean platform for Marine Ecosystem Experimental Research (MEDIMEER) pontoon (43°24′53″N, 3°41′16″E) located on the east side of the lagoon. The mesocosm bags were 280 cm high, with a diameter of 120 cm and an additional 50 cm long sediment trap located at the bottom of the bag. They were made of a transparent nylon-reinforced 200 µm thick vinyl acetate polyethylene film (Insinööritoimisto Haikonen Ky). The emerged part of each mesocosm was covered with a transparent plastic dome to avoid contamination by rain and waves (Fig. 1), making the total structure 300 cm high. The main use of the dome is to prevent precipitations and other external inputs into the mesocosm; however, it allows gas exchange with the atmosphere. The mesocosms were filled with 2200 L of lagoon water.

The water column was gently mixed with a pump (Rule, Model 360), leading to a turnover rate of approximately 3.5 d^{-1}. Each mesocosm unit was equipped with a set of high-frequency automated sensors positioned 1 m deep to measure the DO concentration with an oxygen optode (Oxygen optode 3835, Aanderaa), the conductivity with an electromagnetic induction conductivity sensor (Conductivity sensor 4319, Aanderaa), and the incident photosynthetically active radiation (PAR) with a spherical underwater quantum sensor (LI-193, Li-Cor). Additionally, the water temperature was measured by three temperature sensors (Campbell Scientific Thermistor probe 107) placed at three different depths (0.5, 1, and 1.5 m). For the present study, only the data measured by the oxygen optode and the conductivity, temperature, and incident PAR sensors were used.

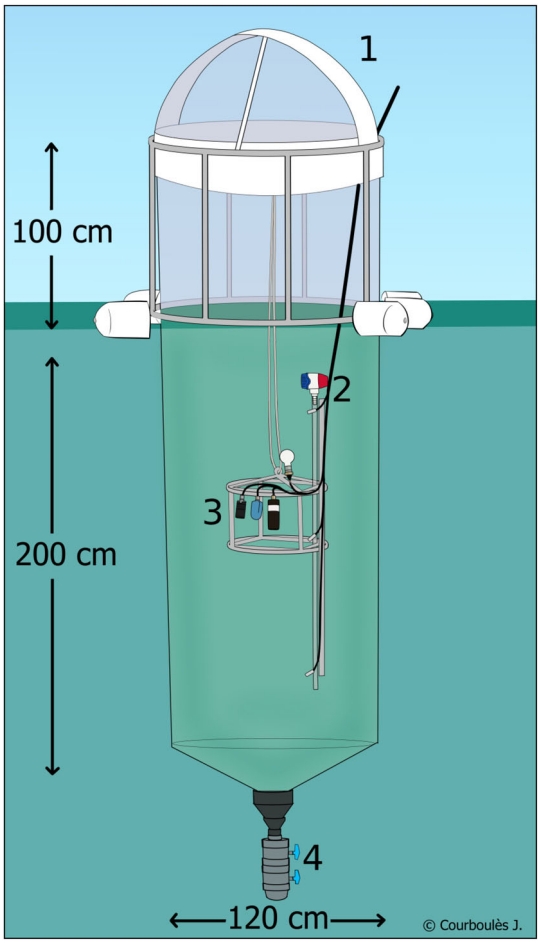

Fig 1. A single mesocosm unit equipped with a dome to cover the structure (1), a pump (2), a sensor system (3), and a sediment trap at the bottom (4) (illustration courtesy of Justine Courboulès).

Estimating metabolic parameters with light and dark incubations using the Winkler method

To compare the metabolic sensor data with data obtained with a classical reference method, Winkler incubations were performed every 2 d. To do so, mesocosm water was sampled using a 5-liter Niskin water sampler. Nine borosilicate bottles of 120 mL were directly filled with water from the Niskin bottle for each mesocosm. The DO contained in three bottles (the t0 bottles) was immediately fixed by adding Winkler reagents as described by Carrit (1966). Three other bottles were carefully wrapped in aluminum foil (the dark bottles) to prevent photosynthesis. These bottles were then incubated in incubation mesocosms along with the three remaining bottles (the light bottles) from 10:00 h to 18:00 h. The two incubation mesocosms were established to incubate light and dark incubation bottles following the Winkler technique as described above. Incubation mesocosms were used to avoid potential contamination and changes in the light environment of the main mesocosms. For the October and June experiments, the incubation mesocosms were located directly adjacent to the other mesocosms and were therefore subject to the same environmental conditions as the control mesocosms. After incubation, the DO in the incubated bottles was fixed as described above. The oxygen concentration in the bottles was measured by using an automated Winkler titrator with a potentiometric

titration method (Crisson titrator and Methrom 916-Ti-touch titrator in the October and June experiments, respectively) (Carpenter 1965).

NCP (in $gO_2\ m^{-3}\ d^{-1}$) was then calculated as in Eq. 1:

$$NCP = \left(\frac{\text{mean}\left(O_{2_{Light}}\right) - \text{mean}(O_{2_{t0}})}{\text{Incubation time}}\right) * \text{dayfraction} * 24 \quad (1)$$

where the mean (O_{2Light}) is the mean value from the triplicate bottles incubated in the light (in $gO_2\ m^{-3}$), the mean (O_{2t0}) is the mean value from the triplicate bottles directly fixed after sampling (in $gO_2\ m^{-3}$), and the day fraction is $\text{dayfraction} = \text{lightperiod}/24$, where the light period refers to the duration from sunrise to sunset in hours.

Respiration (R) (in $gO_2\ m^{-3}\ d^{-1}$) was then calculated as in Eq. 2:

$$R = \left(\frac{\text{mean}(O_{2_{t0}}) - \text{mean}\left(O_{2_{Dark}}\right)}{\text{Incubation time}}\right) * 24 \quad (2)$$

where the mean (O_{2Dark}) is the mean value from the triplicate dark bottles (in $gO_2\ m^{-3}$).

Then, GPP (in $gO_2\ m^{-3}\ d^{-1}$) was obtained as:

$$GPP = NCP + R. \quad (3)$$

Free-water diel oxygen method for metabolic parameter measurements using sensors

Sensor data acquisition and correction

Sensor data were acquired every 1 min in all the mesocosms. The choice of the sampling frequency is very important as useful information to get reliable metabolic estimates could be missed with a slow frequency while a rapid frequency could lead to high amount of data not necessarily needed. This question was addressed and a power analysis assessing the required duration of sensor deployment with sampling frequencies ranging from 1 to 60 min was performed, suggesting that sampling frequencies up to 10 min were sufficient for the 15 d lasting October experiment. This analysis is presented in Appendix 1 in Supporting Information).

Oxygen sensors were calibrated before and after each deployment using three saturation points (0%, 50%, and 100%) and at three different temperatures (17°C, 20°C, and 22°C), according to a calibration procedure described in Bittig et al. (2018). The 100% saturation point was reached by bubbling air into the water, and the 0% and 50% saturation points were reached by adding potassium metabisulfite. The raw DO data measured during the mesocosm experiments were then corrected with the obtained calibration coefficient. Then, the DO data were corrected with the salinity and water temperature data obtained from the conductivity sensors and the temperature probe positioned at 1 m deep, respectively; salinity and temperature correction is required for oxygen optodes in order to take into account variations in O_2 solubility (Bittig et al. 2018). The DO-corrected data were then smoothed using a 9-point moving average. To estimate planktonic metabolism, the smoothed data were then separated into different periods according to the minima and the maxima of the DO curve. Periods between a minimum and the following maximum, indicating that DO was increasing and thus the instantaneous NCP of O_2 was positive, were considered Positive NCP periods. Periods between a maximum and the following minimum, when DO was decreasing and thus the instantaneous NCP was negative, were considered Negative NCP periods. An example of the separation of the data into periods is given for the Oct 01 DO data set in Fig. 2A.

A five-parameter sigmoidal model was built to fit the DO data for each Positive NCP period and each Negative NCP period to reduce short-timescale noise (Mostajir et al. 2013) (SigmaPlot software version 12.3). The initial raw data calibrated and corrected for salinity and temperature, the data smoothed by a 9-point moving average followed by a locally estimated scatterplot smoothing (LOESS) regression, and the data modeled with the five-parameter sigmoidal model are presented in Fig. 2b–d. Outliers in the raw sensor data set were defined as values 20% higher or lower than their direct neighbors and were removed. Consequently, between 0% (Oct 01) and 1.49% (Oct 02) of the initial DO data was removed. Missing values were extrapolated using a linear regression in the local neighborhood of the missing value.

Metabolic parameter calculation

Instantaneous NCP

The governing equation comes from (Odum and Odum 1955), the first application of the method:

$$\frac{\Delta O_2}{\Delta t} = GPP - R - F - A \quad (4)$$

where $\frac{\Delta O_2}{\Delta t}$ is the change in DO concentration during a time interval Δt, GPP is the gross primary production, R is the respiration, F is the exchange of O_2 between the water and the atmosphere, and A is a combined parameter that includes all other phenomena responsible for changes in the DO concentration in the considered system. In this article, A was considered to be negligible.

The exchange between the water surface and the atmosphere, F, was calculated as:

$$F = (k*(O_2 - O_{2_{sat}}))/Z_{mix} \quad (5)$$

where O_2 is the concentration in DO, O_{2sat} is the oxygen saturation, k is the piston velocity coefficient, and Z_{mix} is the mixing depth of the water column, that is, in the present study, the depth of the mesocosms. In this study, k was set to

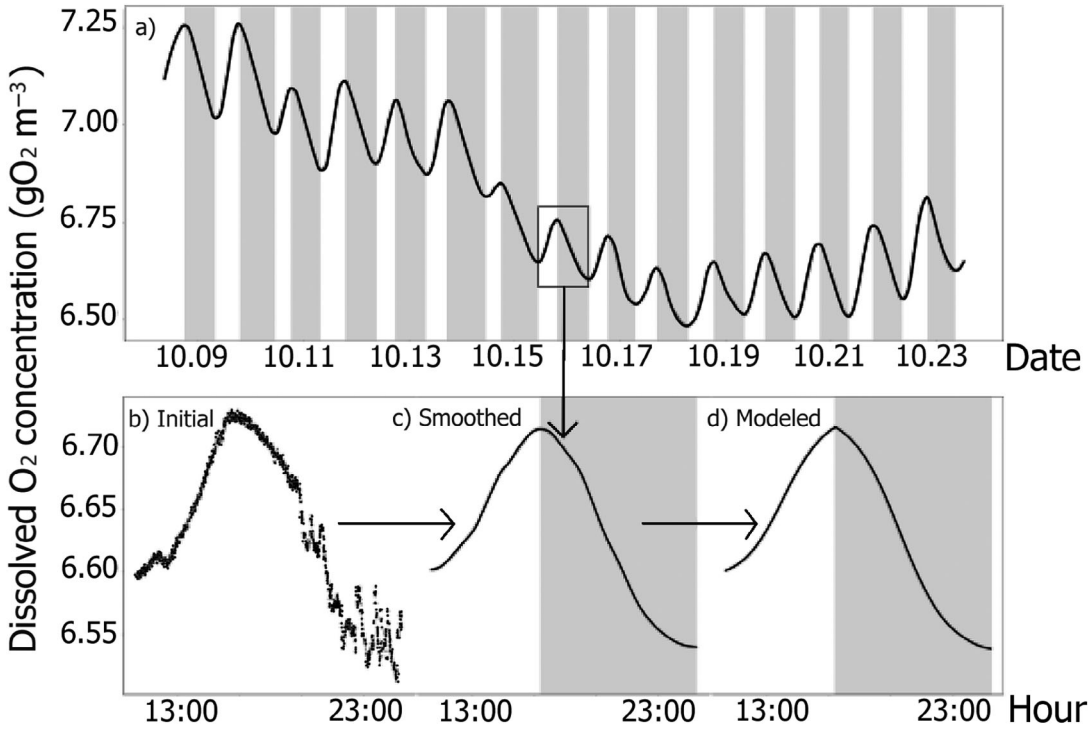

Fig 2. (**a**) Oct 01 smoothed DO data. Shading separates Positive NCP periods (white background) and Negative NCP periods (gray background). The parts in which DO is increasing are considered Positive NCP periods, and the parts in which DO is decreasing are considered Negative NCP periods. The same separation was applied to the data from all the mesocosms. The black rectangle shown in (**a**) is shown in the bottom figure as (**b**), (**c**), and (**d**), corresponding to the initial data (raw data calibrated and corrected for salinity and temperature) (**b**), the smoothed data with a 9-point moving average followed by a LOESS regression (**c**), and the data modeled using a five-parameter sigmoidal model (**d**).

0.000156 m min^{-1}. This value was chosen as it was experimentally measured in open-top laboratory microcosm (Alcaraz et al. 2001) in salinity and temperature conditions close to the conditions of both of the mesocosm experiments used in the present investigation. Moreover, this k value was chosen because it was the lowest value obtained with non-null conditions as our in situ mesocosms naturally experience turbulence due to marine waves. To test eventual differences on metabolic estimates induced by the choice of the k value, a sensitivity analysis using the lowest and the highest value of k measured in similar experimental conditions as in our in situ mesocosms (Alcaraz et al. 2001) was performed and is presented in Appendix 2 in Supporting Information. It appeared that GPP estimates were not significantly sensitive to the choice of the k value. In contrast, significantly higher estimates of R were obtained with the lower k, pointing out that the choice of the k value is more critical for the estimation of R.

For each time step of 1 min, the instantaneous NCP was calculated as:

$$\mathrm{NCP} = \Delta O_2 - F \quad (6)$$

where NCP is the instantaneous net community production of O_2 per minute, ΔO_2 is the difference between two successive DO concentration values, and F is the exchange between the water surface and the atmosphere as previously described.

Instantaneous metabolism values can be integrated over certain periods of the day and the night to obtain daily estimates of GPP, NCP, and R. However, it is still unclear how daily metabolic parameters, notably Rdaytime, should be calculated. Various methods are selected, compared, and presented in the following sections.

Statistical analyses

ANOVAs were used to assess the differences between sensor-based metabolic estimates such as Rdaytime, Rnight, and R24h and to test the effects of the sampling period and the piston velocity coefficient variations on these sensor-based metabolic estimates. A p value less than or equal to 0.05 was considered statistically significant. These analyses were also used to compare the sensor-based metabolic estimates with the estimates obtained with the Winkler method. When the assumptions of ANOVA could not be met even through data transformation (logarithmic, exponential or square-root transformation), a nonparametric Kruskal–Wallis test was used instead. Following the ANOVAs, Tukey honest significant difference (Tukey HSD) tests were used to perform multiple comparisons of means and to test the differences among estimates. Following the Kruskal–Wallis tests, a post hoc nonparametric

Table 1. Presentation of the two methods for estimating Rdaytime and Rnight compared in the present work using certain periods of the instantaneous NCP data.

Data and methods	Rdaytime calculation	Rnight calculation
Sensor data and "max" method (present study)	Mean of instantaneous NCP during a 1-h period centered on the maximum instantaneous negative NCP	Mean of instantaneous NCP for the entire negative NCP period
Sensor data and "Most" method (Mostajir et al. 2013)	Mean of instantaneous NCP during a 1-h period following sunset	Mean of instantaneous NCP for the entire negative NCP period, apart from the period considered in the Rdaytime calculation

Dunn test was performed. All statistical analyses were performed using the *R* software (version 3.4.2).

Estimation of *R* during the day (Rdaytime), at night (Rnight), and daily *R* (R24h), using sensor data

In the present study, as shown in Table 1, Rdaytime, Rnight, and R24h were estimated using sensor data and certain periods of the instantaneous NCP data and were integrated either from sunrise to sunset or only over the production period (e.g., only when the instantaneous NCP was positive). Means of instantaneous NCP over certain time periods were used as in previous studies, including Staehr et al. (2010*a*,*b*), Laas et al. (2012), Idrizag et al. (2016), Richardson et al. (2017), and Chiu et al. (2020). More precisely, Rdaytime was estimated either with the mean of the instantaneous NCP during a 1-h period centered on the maximum of the instantaneous Negative NCP (hereafter referred to as the "Max" method) or with the mean of the instantaneous NCP during a 1-h period following sunset, as in Mostajir et al. (2013) (hereafter referred to as the "Most" method). As the Winkler method is still considered the reference method for estimating planktonic metabolism, the R obtained from sensor data by applying the Max and Most methods were then compared with the R obtained using the Winkler method.

Once the instantaneous Rdaytime and Rnight were calculated as described in Table 1, they were integrated to provide daily values. Two methods of integration were compared. Rdaytime was integrated either over the whole day (e.g., from sunrise to sunset, hereafter referred to as SS) or over the production period (e.g., when instantaneous NCP was positive, hereafter referred to as PP).

When Rdaytime was integrated from sunrise to sunset, Rnight was integrated over the whole night (e.g., from sunset to the following sunrise). When Rdaytime was integrated over the production period, Rnight was integrated over the Negative NCP period.

Therefore, Rdaytime and Rnight were calculated with the following equation:

$$R = (\text{Mean of instantaneous NCP during the considered period}) * 60 * \text{integration period} \quad (7)$$

where R corresponds to either Rdaytime or Rnight ($gO_2\ m^{-3}\ d^{-1}$), the mean of instantaneous NCP is measured in $gO_2\ m^{-3}\ min^{-1}$, and the integration period either to the period from sunrise to sunset (hours) or to the production period (the Positive NCP period, in hours) for Rdaytime calculation, or to the period from sunset to the following sunrise (hours) or to the Negative NCP period (hours) for Rnight calculation. It should be noted that the units of Rdaytime (or Rnight) are indifferently $gO_2\ m^{-3}$ integration $period^{-1}$ or $gO_2\ m^{-3}\ d^{-1}$ because during a given 24 h period, Rdaytime (or Rnight) only occurs during the period in which it is integrated, so its value per 24 h is equal to its value per integration period.

Then, the daily R (R24h) was calculated as the sum of Rdaytime and Rnight. A summary of all the parameters compared in the present work and their designations is presented in Table 2. For the Winkler estimates, the instantaneous Winkler-R was integrated over the Positive NCP period (Rdaytime-Winkler-PP) or from sunrise to sunset (Rdaytime-Winkler-SS) to obtain the daytime R, and it was integrated over the Negative NCP period (Rnight-Winkler-PP) or from sunset to sunrise (Rnight-Winkler-SS) to obtain the night R.

Assessment

Comparison of Rdaytime, Rnight, and R24h estimations from the three different methods and two integration periods

For all mesocosms, the Rdaytime, Rnight, and R24h estimates integrated from sunrise to sunset (SS) and over the PP are presented in Fig. 3. Regardless of their integration period, the Rdaytime estimates were significantly different depending on the method used for their estimation (ANOVA, $p < 10^{-4}$ for all mesocosms and for the two integration periods, Supporting Information Table S1). Rnight estimates were significantly different for three mesocosms out of six (Oct 02, Jun 01, and Jun 03) (ANOVA or Kruskal–Wallis test, $p < 0.05$, Supporting Information Table S1). Consequently, R24h estimates were significantly different for all mesocosms when they were integrated from sunrise to sunset and over the production period. The only exception was in the Oct 01 mesocosm when the estimates were integrated over the production period; these estimates were not significantly different.

Post hoc tests were performed to assess multiple comparisons between estimates and to determine which estimates

Table 2. Presentation of all daily integrated parameters that are compared in the present study.

Parameter	Method	Integrated from sunrise to sunset (SS)	Integrated over the production period (PP)
Rdaytime	Max	Rdaytime-Max-SS	Rdaytime-Max-PP
	Most	Rdaytime-Most-SS	Rdaytime-Most-PP
	Winkler	Rdaytime-Winkler-SS	Rdaytime-Winkler-PP
Rnight	Max	Rnight-Max-SS	Rnight-Max-PP
	Most	Rnight-Most-SS	Rnight-Most-PP
	Winkler	Rnight-Winkler-SS	Rnight-Winkler-PP
R24h	Max	R24h-Max-SS	R24h-Max-PP
	Most	R24h-Most-SS	R24h-Most-PP
	Winkler	R24h-Winkler	R24h-Winkler

were significantly different. For all mesocosms, and regardless of the integration period considered, Rdaytime-Max was significantly higher than Rdaytime-Most (between 75% and 198% higher, depending on the period of integration and on the mesocosm). For both integration periods, Rdaytime-Winkler was significantly higher than Rdaytime-Most for the October mesocosms (on average 150.2%) and significantly lower than Rdaytime-Max for the June mesocosms (on average −61.6%). However, for Rnight, the Max, Most, and Winkler methods gave similar estimates, with only one exception (Rnight-Max-PP was significantly different from Rnight-Winkler-PP for Oct 02). As a result of the differences in Rdaytime and Rnight, R24h-Max was generally significantly higher than R24h-Most. The only exceptions were for Jun 03 integrated over the production period and for Oct 02 and Oct 03 integrated from sunrise to sunset. In contrast, R24h-Winkler was systematically lower than R24h-Max and R24h-Most for all June mesocosms, whereas it was significantly higher than R24h-Most for the Oct 02 and Oct 03 mesocosms. Notably, R24h-Most-PP was on average 1.43, 1.47, and 1.58 times higher than R24h-Winkler for Jun 01, Jun 02, and Jun 03, respectively.

The comparisons reported earlier were performed for the entire experiments. In addition, day-by-day comparisons were also performed and are presented in the Supporting Information Table S2. Generally, the day-by-day comparisons had the same results as reported for the entire experiment. However, occasionally, the difference between Rdaytime-Max and Rdaytime-Most was not significant, as the periods considered for the Max and the Most methods were almost the same. An example is given in Fig. 4: on day 11 in Jun 01, Rdaytime-Max was only 48.9% higher than Rdaytime-Most (Fig. 4b), unlike on day 4 in Oct 01, when Rdaytime-Max was 100.6% higher than Rdaytime-Most (Fig. 4a). The greatest discrepancy between Rdaytime-Max and Rdaytime-Most was found on day 14 of Oct 02 (485.4%), while the smallest difference was on day 14 of Jun 02 (34.8%).

To assess whether the integration period significantly affected the results for Rdaytime, Rnight, and R24h, comparisons were also performed between integration periods (e.g., from sunrise to sunset or over the production period) (Table 3). The ANOVA and Kruskal–Wallis test results showed nonsignificant differences in October, while the values of Rdaytime and Rnight were significantly different in June (Table 3). More precisely, Rdaytime-Max-SS was between 4% and 36% higher than Rdaytime-Max-PP. The observed differences were similar when the Most method was used.

A new method of estimating Rdaytime, Rnight, R24h, GPP, and NCP using sensor data

Regardless of the integration period, Rdaytime-Max was significantly higher than Rdaytime-Most, as demonstrated above. As numerous studies have shown that light respiration is substantially higher than dark respiration (Markager et al. 1992; Pringault et al. 2007; Tobias et al. 2007), we suggest using the new method presented in this investigation, called the "Max method," to estimate Rdaytime, Rnight, and therefore R24h.

Moreover, as demonstrated above, major discrepancies were introduced into the respiration estimates for the Jun experiment by the integration period (SS vs. PP). Thus, we also suggest integrating Rdaytime over the production period, as this method enables us to consider only the period in which production is higher than respiration and therefore is representative of the most productive period of the day. In the same way, we suggest that Rnight be integrated over the Negative NCP period (e.g., when the DO concentration is decreasing).

Hence, based on the sensor data, we suggest calculating Rdaytime, Rnight, R24h, GPP. and NCP as presented in Eqs. 8, 9, 10, 11, and 12 respectively:

$$\text{Rdaytime} = (\text{mean instantaneous NCP during Max period}) \text{ *60*duration of Production Period} \quad (8)$$

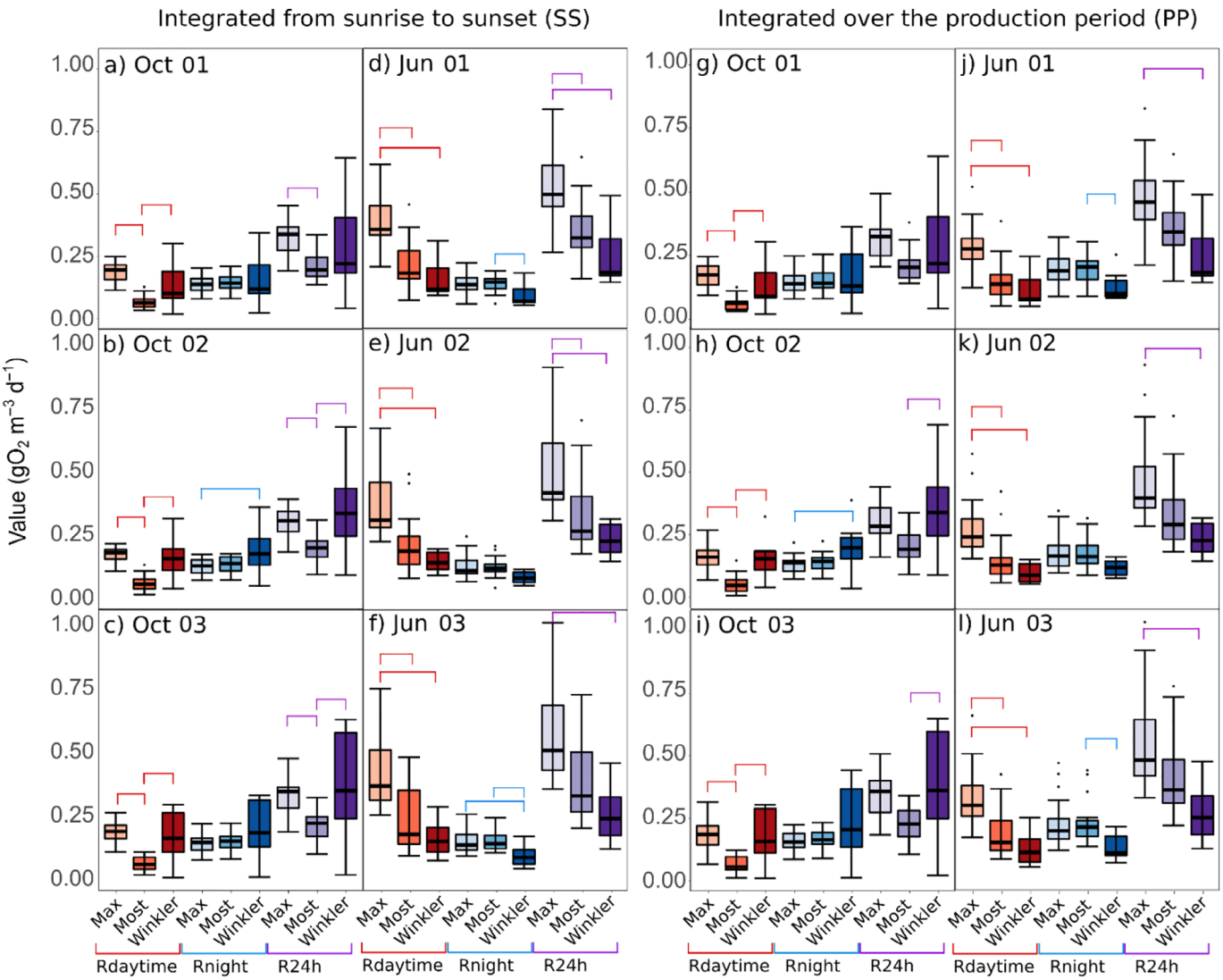

Fig 3. Estimates of Rdaytime (the three leftmost boxplots in orange), Rnight (the three boxplots in blue in the middle), and R (the three rightmost boxplots in purple) obtained from sensor data using the Max and Most methods and from Winkler incubation data integrated from sunrise to sunset or over the production period for Oct 01 (**a**, **g**), Oct 02 (**b**, **h**), Oct 03 (**c**, **i**), Jun 01 (**d**, **j**), Jun 02 (**e**, **k**), and Jun 03 (**f**, **l**). For each box, the lower quartile, median, and upper quartile values are displayed with horizontal lines. Whiskers show the range of the data, from the minimum to the maximum, excluding outliers. Brackets represent the comparisons between estimates that were found to be significantly different ($p < 0.05$, Tukey HSD or Dunn test). Oct 01, Oct 02, and Oct 03 refer to the mesocosms no.1, no.2, and no.3 of the October 2018 experiment, and similarly Jun 01 Jun 02, and Jun 03 refer to the mesocosms no.1, no.2, and no.3 of the May and June 2019 experiment.

where Rdaytime is measured in $gO_2\ m^{-3}\ d^{-1}$, the Max period is a 1-h period centered on the maximum instantaneous Negative NCP, the mean instantaneous NCP is measured in $gO_2\ m^{-3}\ min^{-1}$, and the duration of the production period is the duration of the Positive NCP period in hours.

$$\text{Rnight} = (\text{mean instantaneous NCP during Night period}) \text{*60*duration of Night Period} \quad (9)$$

where Rnight is measured in $gO_2\ m^{-3}\ d^{-1}$, the Night period refers to the Negative NCP period, the mean instantaneous NCP is measured in $gO_2\ m^{-3}\ min^{-1}$, and the duration of the night period is the duration of the Negative NCP period in hours.

R24h is calculated as:

$$\text{R24h} = \text{Rdaytime} + \text{Rnight} \quad (10)$$

Hence, GPP is calculated as follows:

$$\text{GPP} = \text{mean of instantaneous NCP during the Positive NCP period*60*duration of Production Period} + \text{Rdaytime} \quad (11)$$

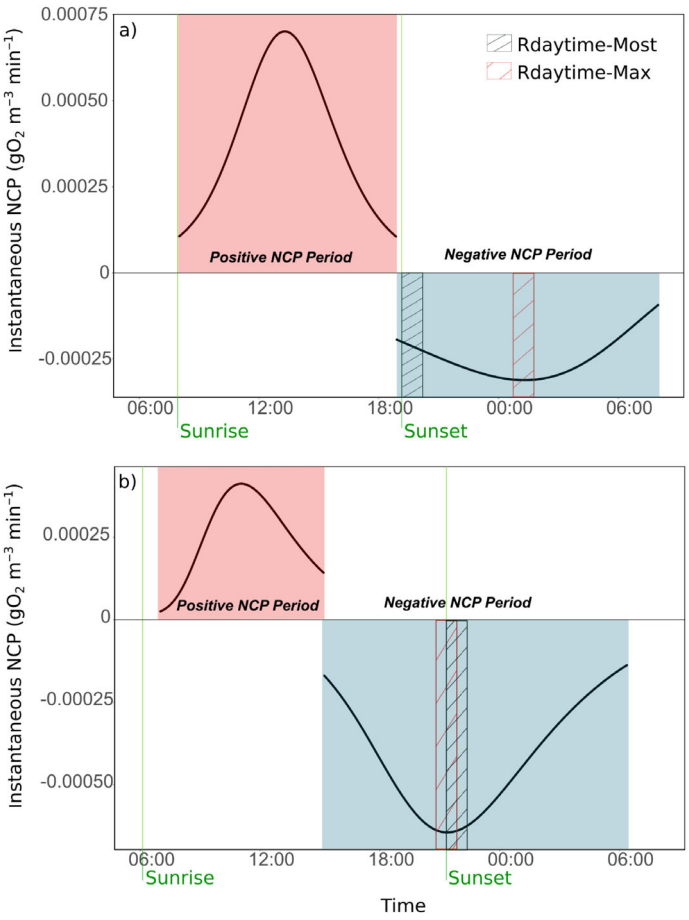

Fig 4. Instantaneous NCP during the Positive and the Negative NCP periods on (**a**) day 4 (11 October 2018) in Oct 01 and (**b**) day 11 (05 June 2019) in Jun 01. The sunrise and sunset times are shown as vertical green lines. The Positive NCP period is represented by a red rectangle, and the Negative NCP period is represented by a blue rectangle. The periods considered for the Rdaytime-Most and Rdaytime-Max calculations are shown as black and red striped rectangles, respectively. The gap between the instantaneous NCP during the Positive NCP period and during the Negative NCP period is a consequence of modeling the DO curve separately for each Positive NCP period and for each Negative NCP period.

where GPP and Rdaytime are measured in $gO_2\ m^{-3}\ d^{-1}$, and the duration of the production period is the duration of the Positive NCP period in hours.

Finally, NCP is calculated as follows:

$$NCP = GPP - R24h \quad (12)$$

Discussion

A computation of daytime respiration that takes into account variations in the coupling of the day–night and O_2 cycles

As discussed before, it has been shown that planktonic daytime respiration is significantly higher than night respiration. Therefore, in the present work, Rdaytime is proposed to be estimated with the maximum instantaneous respiration that can be measured at night. With this method, an average Rdaytime ranging from 23% to 58% higher than Rnight was obtained; this range is consistent those in with previous studies calculated using other methods, as previously noted.

In the present study, the Rdaytime estimated with this new method, using the maximal respiration at night (i.e., the Max method) was compared with the method proposed by Mostajir et al. (2013) (i.e., the Most method). For all mesocosms and regardless of the integration period considered, the Rdaytime obtained with the Max method was generally significantly higher than the Rdaytime obtained with the Most method. This means that respiration directly after sunset had not reached its maximum value yet in most cases. However, on some long, warm days (in the present work, in June, when days were more than 15 h long), the DO cycle does not perfectly match the day–night cycle (e.g., the DO concentration starts to increase sometime after sunrise and/or starts to decrease some time before sunset; Fig. 4b), resulting in Rdaytime-Most and Rdaytime-Max being equivalent. In these cases, the mismatch observed between the DO and the day–night cycles occurred because more DO was consumed

Table 3. Summary table of the *p* values obtained for the one-way ANOVA comparisons between Rdaytime, Rnight, and R24h obtained with the Max and Most methods integrated from sunrise to sunset or over the production period. When the assumptions for a parametric test were not met, a Kruskal–Wallis test was used instead. *p* values lower than 0.05 were considered significant and are presented in bold (*$p < 0.05$, **$p < 0.01$).

Estimate	Test	Oct 01	Oct 02	Oct 03	Jun 01	Jun 02	Jun 03
Rdaytime	Max-SS × Max-PP	0.43	0.51	0.76	**0.01***	**0.02***	**0.03***
	Most-SS × Most-PP	0.61	0.68	0.82	0.09	0.12	0.15
Rnight	Max-SS × Max-PP	0.53	0.64	0.70	**0.006****	**0.02***	**0.03***
	Most-SS × Most-PP	0.53	0.63	0.67	**0.001****	**0.009****	**0.008****
R24h	Max-SS × Max-PP	0.92	0.86	0.99	0.49	0.33	0.52
	Most-SS × Most-PP	0.81	0.87	0.78	0.92	0.88	0.71

through respiration than was produced through photosynthesis, even though the irradiance was still strong in the middle of the afternoon. This phenomenon can be explained by several factors, including a decrease in O_2 production from photosynthesis due to photoinhibition induced by the high irradiance level (Powles 1984) or an increase in bacterial and phytoplankton respiration due to warmer conditions (Jones 1977; Robinson 2008). These variations in the coupling of the day–night and O_2 cycles were not taken into account in previous methods of estimating Rdaytime, whereas the Max method proposed in this article considers them.

As Rdaytime is used to calculate GPP estimates, they were significantly different when estimated with the Max and the Most methods, and are presented in Supporting Information Table S4. The Max method resulted in GPP estimates between 32.6% and 50.5% higher in average than those estimated with the Most method, depending on the mesocosm and the integration period considered. As Rdaytime is also used for the R24h calculation (the total daily respiration), the R24h estimates obtained with the Max method were, similarly to GPP, between 48.2% and 55.8% compared to those obtained with the Most method. As a consequence, daily NCP estimates, which represent the balance between GPP and R24h, were not significantly different using the Max or the Most methods. Therefore, even if one method is underestimating both GPP and R24h comparing to the other, because it is to the same extent, the global oxygen balance is not significantly different.

Patterns in the nighttime data

Dark, or night, respiration by phytoplankton can be basically separated into three distinct phases (Markager and Sand-Jensen 1989; Markager et al. 1992; Mantikci et al. 2017). The first phase corresponds to the direct enhancement of respiration by photosynthesis and lasts for only a few minutes after the onset of darkness. This period is followed by a second phase in which respiration is still higher than basal maintenance respiration due to the intracellular substrate pool created during the previous light exposure (Mantikci et al. 2017, 2019) and lasts for several hours (from 2.5 to 3.6 h; Falkowski et al. 1985; Sadro et al. 2011). Moreover, the duration of this light-enhanced respiration period is season-dependent, with longer durations in the months with longer daylengths (Sadro et al. 2011). This phase is also dependent on the substrate pool available for phytoplankton and must be differentiated from the final phase, which represents basal maintenance respiration (Mantikci et al. 2017). However, in the present study, the durations of the second phase (e.g., between the start of the Negative NCP period, when respiration starts to be higher than O_2 production, and the point of maximum instantaneous respiration) in October and June were similar (Supporting Information Table S3). This phase includes a period in which production is still occurring but is lower than respiration (between the start of the Negative NCP period and sunset, see Fig. 4b). The latter phase was several hours longer in June than in October because the DO concentration started to decrease well before sunset in June. Consequently, the period in which only respiration occurs (e.g., from sunset to the point of maximum respiration) was longer in October than in June, and its duration is in line with those measured in previous studies (Falkowski et al. 1985; Markager and Sand-Jensen 1989; Sadro et al. 2011).

Moreover, the respiration pattern observed in the present investigation encompasses also heterotrophic respiration, and not only phytoplanktonic one. Bacterial respiration depends on other types of substrates, and does not necessarily vary throughout day and night the same way phytoplanktonic respiration does. An increasing respiration rate during dark conditions was found for a planktonic population dominated by bacteria (e.g., a planktonic community after a phytoplankton bloom). This increase in respiration during a dark period was proposed to be related to an increase in bacteria biomass and production (Briand et al. 2004). Overall, the nighttime respiration pattern gives information about the dominant respiratory processes in the studied system (Mantikci et al. 2019). Indeed, the nighttime respiration pattern varies accordingly to the quality and the quantity of organic substrates available, as well as the distribution of the global respiration between heterotrophic and autotrophic organisms. In a system with different characteristics than that of the present study, respiration patterns may be very different from the ones observed in the present investigation.

Comparison between sensor data and Winkler data

The values of Rdaytime, Rnight, and R24h estimated by the Winkler method, which were normalized on the same period as those obtained with the Max and the Most methods, were sometimes significantly different from those obtained using sensor data. These discrepancies are in accordance with Mostajir et al. (2013), who obtained Winkler respiration rates that were three times lower than sensor respiration rates. These discrepancies may be due to several fundamental differences between the two methods. First, the Winkler method requires the confinement of the plankton community in small, closed bottles (several hundred milliliters). As a result, the metabolism estimated in the glass bottles might not be representative of the mesocosm (several m^3). Additionally, the plankton community must acclimate to its new confined environment, leading to potential differences between the metabolism of the community in the incubation glass bottles and that of the natural or mesocosm waters. This so-called "bottle effect" has long been noted as a potential bias in metabolism estimation using the Winkler technique (Bender et al. 1987). Moreover, to measure respiration, Winkler incubations are typically performed during the day or under light exposure, with bottles covered to prevent light and thus photosynthesis (Smith and Kemp 1995; Liess et al. 2016; Mesa et al. 2017). Therefore, Winkler respiration values are obtained from a

community that is acclimated to natural light conditions and is suddenly put in the dark. Thus, the organisms must instantaneously change their metabolism without an acclimation period, which creates a source of bias in respiration measurements. In contrast, the sensors installed in the mesocosms allow us to measure the plankton community's metabolic parameters in a noninvasive way, directly in their quasi-natural environment, with natural light conditions during the day and at night.

Comparison of two integration periods for the sensor data

The discrepancies between the daily Rdaytime estimates integrated from sunrise to sunset and those integrated over the production period were greater when the daylength was longer (i.e., in June in the present study). This is because, even if the daylength varies, the production period is still comparable across seasons (Supporting Information Table S3). This characteristic of the production period may be explained by the fact that metabolic processes are controlled by various mechanisms, such as temperature variations, throughout the seasons and not only by the daylength and the amount of light received (Solomon et al. 2013; Alfonso et al. 2018; Lopez Sandoval et al. 2019). As a result, during long days, the actual production period is considerably shorter than the daylength, and hence Rdaytime integrated over the production period is in fact integrated over a significantly shorter period than that integrated from sunrise to sunset. Rnight estimates were also significantly different between the two integration periods but in the opposite way as Rdaytime estimates; the Rnight estimates integrated from sunset to the following sunrise are integrated over a shorter period than those integrated over the entire Negative NCP period. Consequently, R24h was not significantly affected by the integration period, as the differences induced in both Rdaytime and Rnight were equal to each other. Hence, when comparing Rdaytime estimates obtained in different seasons, the estimates should be integrated over comparable time periods, but the integration time period is less important in studies focusing only on R24h.

Comments and recommendations

In situ mesocosm experiments are a useful approach in aquatic ecology because they allow the assessment and quantification of the responses of planktonic and microbial communities to various perturbations within a controlled environment under in situ conditions. The ability of these experiments to effectively mirror in situ conditions has been investigated often; although there are some discrepancies between the biotic and abiotic parameters of mesocosms and those of the ecosystem they are deployed in, mesocosms still represent one of the best experimental ways to address certain fundamental questions in aquatic ecology (Dzialowski et al. 2014). However, mesocosm experiments often require a meticulous, time-consuming, and labor-intensive sampling effort to obtain enough data to be able to monitor several key parameters, such as oxygen concentrations. High-frequency automated sensors can be used to monitor these parameters in a more efficient and easier way, as they need only to be deployed at the beginning of the experiment and retrieved at the end. Data generated via these sensors can be used to obtain valuable insights into the responses of the system to the tested perturbation(s), notably by assessing the metabolism of the system. As mentioned before, this method has many advantages compared to classical methods; however, it also has a few limitations and uncertainties. One of the limitations is the dependence of the method on a reliable estimate of the air–water exchange coefficient. This is combined with the fact that physical phenomena and their contributions to DO variability may vary greatly depending on both the tested ecosystem and the mesocosm structure. These physical aspects should be the focus of future research. Nevertheless, the goal of mesocosm experiments is to compare control mesocosms with mesocosms in which one or more disturbance(s) were applied. In this context, an over- or underestimated piston velocity coefficient will not have a substantial impact on the measured responses of the treatment compared to control mesocosms as long as the same piston velocity coefficient is used for all mesocosms.

Another limitation of this method is that it relies on strong daily DO cycles in order to be applicable. Therefore, this method is fully applicable in locations with pronounced day–night cycles, and it might be challenging to apply in low-production systems, like turbid rivers and estuaries. However, this method becomes more challenging to apply at latitudes where the cycle is less marked and impossible to apply when DO does not have a daily cycle. This means that the method can be used to calculate instantaneous NCP during only certain months of the year in polar ecosystems, as it is not possible to estimate both GPP and R without DO cycles.

To conclude, in the present study, we presented a reliable method of estimating daytime respiration developed using automated sensors in in situ mesocosms. This method takes into account the variability of the coupling between day–night and O_2 cycles and therefore provides a better assessment of planktonic metabolic parameters than other methods. We also provide recommendations about various aspects of the technique, such as the measurement frequency to use and the physical air–water exchange of oxygen.

Mesocosm studies investigating the responses of aquatic communities to environmental stress should move toward the use of devices that are more autonomous and less costly in terms of time, work, and price than classical methods. The use of high-frequency sensors in mesocosms is one way to achieve this goal. By addressing certain methodological questions regarding the use of the free-water diel oxygen technique for in situ enclosed mesocosm experiments, this work improves our ability to assess high-frequency instantaneous metabolism and consequently the metabolic responses of communities to

disturbance and establishes a common protocol for data analysis.

References

Alcaraz, M., C. Marrasé, F. Peters, L. Arin, and A. Malits. 2001. Seawater–atmosphere O2 exchange rates in open-top laboratory microcosms: application for continuous estimates of planktonic primary production and respiration. J. Exp. Mar. Biol. Ecol. **257**: 1–12. doi:10.1016/S0022-0981(00)00328-2

Alfonso, M. B., A. S. Brendel, A. J. Vitale, C. Seitz, M. C. Piccolo, and G. M. E. Perillo. 2018. Drivers of ecosystem metabolism in two managed shallow lakes with different salinity and trophic conditions: The Sauce Grande and La Salada Lakes (Argentina). Water **10**: 1136. doi:10.3390/w10091136

Alkire, M. B., and others. 2012. Estimates of net community production and export using high-resolution, Lagrangian measurements of O_2, NO_3^-, and POC through the evolution of a spring diatom bloom in the North Atlantic. Deep-Sea Res. I Oceanogr. Res. Pap. **64**: 157–174. doi:10.1016/j.dsr.2012.01.012

Beardall, J., T. Burger-Wiersma, M. Rijkeboer, A. Sukenik, J. Lemoalle, Z. Dubinsky, and D. Fontvielle. 1994. Studies on enhanced post-illumination respiration in microalgae. J. Plankton Res. **16**: 1401–1410. doi:10.1093/plankt/16.10.1401

Bender, M., and others. 1987. A comparison of four methods for determining planktonic community production. Limnol. Oceanogr. **32**: 1085–1098. doi:10.4319/lo.1987.32.5.1085

Bittig, H. C., and others. 2018. Oxygen optode sensors: Principle, characterization, calibration, and application in the ocean. Front. Mar. Sci. **4**: 429. doi:10.3389/fmars.2017.00429

Briand, E., O. Pringault, S. Jacquet, and J. P. Torreton. 2004. The use of oxygen microprobes to measure bacterial respiration for determining bacterioplankton growth efficiency. Limnol. Oceanogr. **2**: 406–416. doi:10.4319/lom.2004.2.4066

Briggs, N., K. Guðmundsson, I. Cetinić, E. D'Asaro, E. Rehm, C. Lee, and M. J. Perry. 2018. A multi-method autonomous assessment of primary productivity and export efficiency in the springtime North Atlantic. Biogeosciences **15**: 4515–4532. doi:10.5194/bg-15-4515-2018

Brinkman, A. G., C. J. M. Philippart, and A. F. Zuur. 1995. Model methods for the analysis of mesocosm experimental studies. Helgoländer Meeresuntersuchungen **49**: 771–784. doi:10.1007/BF02368400

Carpenter, J. H. 1965. The accuracy of the Winkler method for dissolved oxygen analysis. Limnol. Oceanogr. **10**: 135–140. doi:10.4319/lo.1965.10.1.0135

Carrit, D. E. 1966. Comparison and evaluation of currently employed modifications of the Winkler method for determining oxygen in seawater. A NASCO report. J. Mar. Res. **24**: 286–318.

Carvalho, M. C., and B. D. Eyre. 2012. Measurement of planktonic CO_2 respiration in the light. Limnol. Oceanogr.: Methods **10**: 167–178. doi:10.4319/lom.2012.10.167

Chiu, C.-Y., and others. 2020. Terrestrial loads of dissolved organic matter drive inter-annual carbon flux in subtropical lakes during times of drought. Sci. Total Environ. **717**. doi:10.1016/j.scitotenv.2020.137052

Crossland, N. O., and T. W. L. Point. 1992. The design of mesocosm experiments. Environ. Toxicol. Chem. **11**: 1–4. doi:10.1002/etc.5620110101

de Eyto, E., and others. 2019. High frequency monitoring reveals fine scale spatial and temporal dynamics of the deep chlorophyll maximum of a stratified coastal lagoon. Estuar. Coast. Shelf Sci. **218**: 278–291. doi:10.1016/j.ecss.2018.12.010

Demars, B. O. L., J. Thompson, and J. R. Manson. 2018. Stream metabolism and the open diel oxygen method: Principles, practice, and perspectives. Limnol. Oceanogr.: Methods **13**: 356–374. doi:10.1002/lom3.10030

Dzialowski, A. R., M. Rzepecki, I. Kostrzewska-Szlakowska, K. Kalinowska, A. Palash, and J. T. Lennon. 2014. Are the abiotic and biotic characteristics of aquatic mesocosms representative of in situ conditions? J. Limnol. **73**: 603–612. doi:10.4081/jlimnol.2014.721

Falkowski, P. G., Z. Dubinsky, and G. Santostefano. 1985. Light-enhanced dark respiration in phytoplankton. SIL Proc. 1922-2010 **22**: 2830–2833. doi:10.1080/03680770.1983.11897784

Hanson, P. C., D. L. Bade, S. R. Carpenter, and T. K. Kratz. 2003. Lake metabolism: Relationships with dissolved organic carbon and phosphorus. Limnol. Oceanogr. **48**: 1112–1119. doi:10.4319/lo.2003.48.3.1112

Hanson, P. C., S. R. Carpenter, N. Kimura, C. Wu, S. P. Cornelius, and T. K. Kratz. 2008. Evaluation of metabolism models for free-water dissolved oxygen methods in lakes. Limnol. Oceanogr.: Methods **6**: 454–465. doi:10.4319/lom.2008.6.454

Hensley, R. T., and M. J. Cohen. 2020. Nitrate depletion dynamics and primary production in riverine benthic chambers. Freshw. Sci. **39**: 169–182. doi:10.1086/707650

Hotchkiss, E. R., and R. O. Hall Jr. 2014. High rates of daytime respiration in three streams: Use of $\delta^{18}O_{O2}$ and O_2 to model diel ecosystem metabolism. Limnol. Oceanogr. **59**: 798–810. doi:10.4319/lo.2014.59.3.0798

Idrizag, A., A. Laas, U. Anijalg, and P. Noges. 2016. Horizontal differences in ecosystem metabolism of a large shallow lake. J. Hydrol. **535**: 93–100. doi:10.1016/j.jhydrol.2016.01.037

Jones, R. I. 1977. The importance of temperature conditioning to the respiration of natural phytoplankton

communities. Br. Phycol. J. **12**: 277–285. doi:10.1080/00071617700650291

Kritzberg, E. S., W. Granéli, J. Björk, C. Brönmark, P. Hallgren, A. Nicolle, A. Persson, and L.-A. Hansson. 2014, Warming and browning of lakes: consequences for pelagic carbon metabolism and sediment delivery. Freshw Biol. **59**: 325–336. doi:10.1111/fwb.12267

Laas, A., Noges, P., Koiv, T., and Noges, T. 2012. High-frequency metabolism study in a large and shallow temperate lake reveals seasonal switching between net autotrophy and net heterotrophy. Hydrobiologia **694**: 57–74. doi:10.1007/s10750-012-1131-z

Lauster, G. H., P. C. Hanson, and T. K. Kratz. 2006. Gross primary production and respiration differences among littoral and pelagic habitats in northern Wisconsin lakes. Can. J. Fish. Aquat. Sci. **63**: 1130–1141.

Leclercq, N., J.-P. Gattuso, and J. Jaubert. 1999. Measurement of oxygen metabolism in open-top aquatic mesocosms: Application to a coral reef community. Mar. Ecol. Prog. Ser. **177**: 299–304. doi:10.3354/meps177299

Liess, A., and others. 2016. Terrestrial runoff boosts phytoplankton in a Mediterranean coastal lagoon, but these effects do not propagate to higher trophic levels. Hydrobiologia **766**: 275–291. doi:10.1007/s10750-015-2461-4

Lopez Sandoval, D., K. Rowe, P. Carillo-de-Albonoz, C. M. Duarte, and S. Agusti. 2019. Rates and drivers of Red Sea plankton community metabolism. Biogeosciences **16**: 2983–2995. doi:10.5194/bg-16-2983-2019

Mantikci, M., J. L. S. Hansen, and S. Markager. 2017. Photosynthesis enhanced dark respiration in three marine phytoplankton species. J. Exp. Mar. Biol. Ecol. **497**: 188–196. doi:10.1016/j.jembe.2017.09.015

Mantikci, M., P. A. Staerh, J. L. S. Hansen, and S. Markager. 2019. Patterns of dark respiration in aquatic systems. Mar. Freshw. Res. **71**: 432–442. doi:10.1071/MF18221

Markager, S., and K. Sand-Jensen. 1989. Patterns of night-time respiration in a dense phytoplankton community under a natural light regime. J. Ecol. **77**: 49. doi:10.2307/2260915

Markager, S., A.-M. Jespersen, T. V. Madsen, E. Berdalet, and R. Weisburd. 1992. Diel changes in dark respiration in a plankton community, p. 119–130.*In* T. Berman, H. J. Gons, and L. R. Mur [eds.], The daily growth cycle of phytoplankton: Proceedings of the fifth International Workshop of the Group for Aquatic Primary Productivity (GAP), held at Breukelen, The Netherlands 20–28 April 1990. Springer.

Mesa, E., and others. 2017. Continuous daylight in the high-Arctic summer supports high plankton respiration rates compared to those supported in the dark. Sci. Rep. **7**: 1247. doi:10.1038/s41598-017-01203-7

Mostajir, B., E. Le Floc'h, S. Mas, R. Pete, D. Parin, J. Nouguier, E. Fouilland, and F. Vidussi. 2013. A new transportable floating mesocosm platform with autonomous sensors for real-time data acquisition and transmission for studying the pelagic food web functioning. Limnol. Oceanogr.: Methods **11**: 394–409. doi:10.4319/lom.2013.11.394

Odum, E. P. 1984. The mesocosm. Bioscience **34**: 558–562. doi:10.2307/1309598

Odum, H. T. 1956. Primary production in flowing waters. Limnol. Oceanogr. **1**: 102–117. doi:10.4319/lo.1956.1.2.0102

Odum, H. T., and E. P. Odum. 1955. Trophic structure and productivity of a windward coral reef community on Eniwetok Atoll. Ecol. Monogr. **25**: 291–320. doi:10.2307/1943285

Oviatt, C., M. Pilson, S. Nixon, J. Frithsen, D. Rudnick, J. Kelly, J. Grassle, and J. Grassle. 1984. Recovery of a polluted estuarine system: A mesocosm experiment. Mar. Ecol. Prog. Ser. **16**: 203–217. doi:10.3354/meps016203

Oviatt, C., A. Keller, P. Sampou, and L. Beatty. 1986. Patterns of productivity during eutrophication: A mesocosm experiment. Mar. Ecol. Prog. Ser. **28**: 69–80. doi:10.3354/meps028069

Powles, S. B. 1984. Photoinhibition of photosynthesis induced by visible light. Annu. Rev. Plant Physiol. **35**: 15–44. doi:10.1146/annurev.pp.35.060184.000311

Pringault, O., V. Tassas, and E. Rochelle-Newall. 2007. Consequences of respiration in the light on the determination of production in pelagic systems. Biogeosciences **4**: 105–114.

Reijo, C. J., R. T. Hensley, and M. J. Cohen. 2018. Isolating stream metabolism and nitrate processing at point-scales, and controls on heterogeneity. Freshw. Sci. **37**: 238–250. doi:10.1086/697319

Richardson, D. C., C. C. Carey, D. A. Bruesewitz, and K. C. Weathers. 2017. Intra- and inter-annual variability in metabolism in an oligotrophic lake. Aquat. Sci. **79**: 319–333. doi:10.1007/s00027-016-0499-7

Robinson, C. 2008. Heterotrophic bacterial respiration, p. 299–334.*In* D. L. Kirchman [ed.], Microbial ecology of the oceans. Wiley.

Sadro, S., C. E. Nelson, and J. M. Melack. 2011. Linking diel patterns in community respiration to bacterioplankton in an oligotrophic high-elevation lake. Limnol. Oceanogr. **56**: 540–550. doi:10.4319/lo.2011.56.2.0540

Smith, E., and W. Kemp. 1995. Seasonal and regional variations in plankton community production and respiration for Chesapeake Bay. Mar. Ecol. Prog. Ser. **116**: 217–231. doi:10.3354/meps116217

Solomon, C. T., and others. 2013. Ecosystem respiration: Drivers of daily variability and background respiration in lakes around the globe. Limnol. Oceanogr. **58**: 849–866. doi:10.4319/lo.2013.58.3.0849

Staehr, P. A., D. Bade, M. C. V. de Bogert, G. R. Koch, C. Williamson, P. Hanson, J. J. Cole, and T. Kratz. 2010a. Lake metabolism and the diel oxygen technique: State of the science. Limnol. Oceanogr.: Methods **8**: 628–644. doi:10.4319/lom.2010.8.0628

Staehr, P. A., K. Sand-Jensen, A. L. Raun, B. Nilsson, and J. Kidmose. 2010b. Drivers of metabolism and net heterotrophy in contrasting lakes. Limnol. Oceanogr. **55**: 817–830. doi:10.4319/lo.2010.55.2.0817

Staehr, P. A., J. M. Testa, W. M. Kemp, J. J. Cole, K. Sand-Jensen, and S. V. Smith. 2012. The metabolism of aquatic ecosystems: History, applications, and future challenges. Aquat. Sci. **74**: 15–29. doi:10.1007/s00027-011-0199-2

Stewart, R. I. A., and others. 2013. Chapter two - Mesocosm experiments as a tool for ecological climate-change research, p. 71–181.*In* G. Woodward and E. J. O'Gorman [eds.], Advances in ecological research. Academic Press.

Tobias, C. R., J. K. Böhlke, and J. W. Harvey. 2007. The oxygen-18 isotope approach for measuring aquatic metabolism in high productivity waters. Limnol. Oceanogr. **52**: 1439–1453. doi:10.4319/lo.2007.52.4.1439

Trombetta, T., F. Vidussi, S. Mas, D. Parin, M. Simier, and B. Mostajir. 2019. Water temperature drives phytoplankton blooms in coastal waters. PLoS One **14**: e0214933. doi:10.1371/journal.pone.0214933

Van de Bogert, M. C., S. R. Carpenter, J. J. Cole, and M. L. Pace. 2007. Assessing pelagic and benthic metabolism using free water measurements. Limnol. Oceanogr.: Methods **5**: 145–155. doi:10.4319/lom.2007.5.145

Whitledge, G. W., and C. F. Rabeni. 2000. Benthic community metabolism in three habitats in an Ozark stream. Hydrobiologia **437**: 165–170.

Wikner, J., S. Panigrahi, A. Nydahl, E. Lundberg, U. Båmstedt, and A. Tengberg. 2013. Precise continuous measurements of pelagic respiration in coastal waters with oxygen optodes. Limnol. Oceanogr.: Methods **11**: 1–15. doi:10.4319/lom.2013.11.1

Winkler, L. W. 1888. Die Bestimmung des in Wasser gelösten Sauerstoffen. Berichte der Deutschen Chemischen Gesellschaft **21**: 2843–2855.

Xue, X., D. A. Gauthier, D. H. Turpin, and H. G. Weger. 1996. Interactions between photosynthesis and respiration in the green alga *Chlamydomonas reinhardtii* (characterization of light-enhanced dark respiration). Plant Physiol. **112**: 1005–1014. doi:10.1104/pp.112.3.1005

Acknowledgments

We would like to thank Rémi Valdès, Solenn Soriano, Kevin Mestre, and Camille Suarez-Bazille, the staff of the Sète Marine Station, for helping with setting up the mesocosms and with daily sampling. We also thank Thomas Trombetta, Emilie Eveque, and Jean-François Thevenot for assistance with the daily sampling and with the oxygen sample analyses. Furthermore, we would like to thank Emilie le Floc'h for commenting the model construction and Justine Courboulès for providing the illustration of the mesocosm system. The research leading to these results and a part of the PhD scholarship awarded to TS were funded under the European Union Horizon 2020 Program (H2020/2017-2020), grant agreement 731065-AQUACOSM: Network of Leading European AQUAtic MesoCOSM Facilities Connecting Mountains to Oceans from the Arctic to the Mediterranean. We would like to acknowledge Robert Ptacnik and Herwig Stibor for their helpful comments on the previous version of the manuscript, as well as other participants of the AQUACOSM European project for the constructive discussions during workshops and meetings.

Conflict of Interest

None declared.

Submitted 29 September 2020
Revised 28 January 2021
Accepted 18 February 2021

Associate editor: Scott Ensign